USING 10-BE TO DETERMINE SEDIMENT PRODUCTION AND TRANSPORT RATES ON STEEP HILLSLOPES IN VARIED TECTONIC AND CLIMATIC SETTINGS

A Thesis Presented

by

Matthew C. Jungers

to

The Faculty of the Graduate College

of

The University of Vermont

In Partial Fulfillment of the Requirements
for the Degree of Master of Science
Specializing in Geology

February, 2008

Accepted by the Faculty of the Graduate College, The University of Vermont, in partial fulfillment of the requirements for the degree of Master of Science, specializing in Geology.

Thesis Examination Committee:

_____ **Advisor**
Paul R. Bierman, Ph.D.

_____
Tom Neumann, Ph.D.

_____ **Chairperson**
Wendy-Sue Harper, Ph. D.

_____ **Vice President for Research**
Frances E. Carr, Ph. D **and Dean of Graduate Studies**

Date: April 13, 2007

ABSTRACT

I seek to quantify sediment production and transport rates on steep, soil-mantled hillslopes. Specifically, I am using the activity of ^{10}Be produced by cosmic ray bombardment, measured in both discrete and amalgamated transect samples of hillslope sediment (an extension of the method of Nichols et al., 2002, 2005), in conjunction with simple models of hillslope behavior, to better understand the patterns and rates of sediment production, as well as rates of sediment movement downslope. I have collected suites of samples (n = 96) from hillslope transects across varied climatic and tectonic settings. I focus on my most complete dataset from the Great Smoky Mountains, NC, for this thesis. These initial data clearly show that the spatial distribution of ^{10}Be in hillslope soil is systematic and thus interpretable. Nuclide concentrations indicate the extent of soil stirring and are consistent with down-slope soil transport.

Sample sites include north-central Pennsylvania, New Zealand's North Island, Great Smoky Mountains National Park, the Oregon Coast Range, and the central plateau of Madagascar. Field and isotopic data from these hillslope samples is being considered along with cosmogenic data from river sediment samples collected near each site. This pairing provides context for the results of my new application of cosmogenic nuclides, and adds breadth and depth to the relevancy of this work and that of our collaborators. The importance of the link between hillslope processes and inferred basin-scale erosion rates is often cited (Bierman and Steig, 1996; Brown et al., 1995; Matmon et al., 2003), but rarely explored quantitatively (Heimsath et al., 2005). My project explicitly makes this link.

The stated goal of this thesis was to develop a method for quantifying rates of sediment production and transport on hillslopes using ^{10}Be; that goal was successfully achieved. My work relies upon the power of amalgamation to both investigate and to smooth spatial variance in ^{10}Be concentrations. Using cosmogenically-produced isotopes as a geomorphic tracer allows me to both quantify soil production and track soil as it is transported downslope. In the Great Smoky Mountains, best-fit models of the data require soil velocities of 1-3 $cm \cdot yr^{-1}$ in the well-mixed active layer of the soil. The thickness of this active transport layer is dependent on the rooting depth of trees on the slope and the related depth of soil turnover and mixing due to treethrow. Modeled soil fluxes range from 55-165 $cm^3 \cdot yr^{-1} \cdot cm^{-1}$ depending on whether soil velocity or the thickness of the actively transported layer is assumed to be constant downslope. Diffusion coefficients calculated from these flux rates range from 82-247 $cm^3 \cdot yr^{-1} \cdot cm^{-1}$. This range of diffusion coefficients is most likely related to climatic variation. This hillslope does not appear to be in steady state, calling into question what constitutes a state of steady erosion for an ancient mountain range such as the Appalachians.

CITATIONS

Material from this thesis will be submitted for publication to *Geology*, in the following form:

Jungers, M.C., Bierman, P.R., Matmon, A., Nichols, K., Larsen, J., and Finkel, R., Deciphering Diffusion: *In situ*-produced ^{10}Be as a Geomorphic Tracer of Hillslope Sediment Production and Transport, Geology.

ACKNOWLEDGEMENTS

I would like to thank my advisor Paul Bierman for his support in completing this project. Paul provided invaluable guidance both in the field and at home. More importantly, though, he's become a lifetime friend and mentor marked by a rare combination of both great intellect and great patience.

Joanna Reuter, Luke Reusser, Ari Matmon, and Fara Rasoazanamparany also assisted me in the field. Each of these people provided both insights into my field areas and good company/strong backs when heavy things needed to be carried. While back at home, Jane Duxbury, Luke Reusser, Colleen Sullivan, Jennifer Larsen, Michala Peabody, and Adam Hunt were a pleasure to work with. I consider myself lucky to have had such a great research group with which to work. The rest of the UVM grad students (past and present) were always good for a laugh or a beer.

Thanks are due to my committee members Wendy-Sue Harper and Tom Neumann for comments on my thesis and project. Arjun Heimsath and Josh Roering served as friendly and informative hillslope soil flux experts from afar when questions about their own research arose.

Final thanks go to my family and friends and of course the lovely Angie Mae for their support when I needed it most.

TABLE OF CONTENTS

LIST OF TABLES

LIST OF FIGURES

CHAPTER 1: INTRODUCTION

Hillslopes are everywhere; we build on them, farm on them, and play on them. However, the specific nature of hillslope processes remains largely enigmatic despite geologists' best research efforts. Ironically, the ubiquity of hillslopes is one of the factors that make them a challenge to study. While the shapes of hillslopes may remain consistent across different regions of the world, the soils that mantle those slopes are unique products of underlying bedrock, glacial history, climate, regional vegetation types and density, and human land-use effects. Hillslope form is then intimately linked to the rate at which soil is being produced, and the rate at which soil is being transported, or eroded, off of the slope. This balance between soil production and soil transport is what defines whether a hillslope is soil-mantled or eroded down to bedrock (Carson, 1972). An understanding of how a slope's soil mantle may, or may not, be maintained over time has important implications for the engineering and agricultural applications mentioned above. Further, the importance of the link between hillslope processes and inferred basin-scale erosion rates is often cited by geomorphologists (Bierman and Steig, 1996; Brown et al., 1995; Matmon et al., 2003a) but rarely explored quantitatively (Heimsath, 2005). My project explicitly makes this link.

I use cosmogenic ^{10}Be to trace soil production and transport on hillslopes across varied climatic and tectonic settings. Measurements of cosmogenic nuclides allow the investigation of hillslope processes on a geologically relevant timescale (millennia), in contrast to previous studies that attempted to make meaningful measurements across just

a few field seasons (Fleming, 1975). There is also a tendency in the study of hillslope form and process to model transport rates based on an assumed proportional link between hillslope gradient and soil flux (Davis, 1892; Gilbert, 1877, 1909; Roering, 1999, 2001a). While these studies have been very important for exploring various soil transport laws, they lack fieldwork-based support for their conclusions. Since this study relies on isotope abundances in soil samples and field observations made during sample collection, I can test soil transport laws and their underlying assumptions. The only requirement for our methods is the presence of quartz in the soil to be sampled.

In order to test the universal applicability of our methods, we sampled across a wide range of climatic and tectonic settings. These settings ranged from the humid temperate climates of the ancient Appalachian Mountains in Pennsylvania and North Carolina, to the tectonically active Oregon Coast Range and North Island of New Zealand. I also sampled the central plateau of Madagascar where precipitation is seasonal and the underlying bedrock is Precambrian. I strove to keep my methods and sampling strategy as uniform as possible, despite differences in each site's landscape. Thus, differences in ^{10}Be concentrations and patterns of ^{10}Be abundance must be the result of characteristics unique to each site, and we can determine whether our methods can resolve soil production and transport methods despite these differences.

The following chapters will begin with a review of the current literature related to hillslope processes to provide context for my work. For my thesis, I focus on my work in the Great Smoky Mountains, NC. This North Carolina field area is covered in detail by a paper prepared for submission to Geology. Descriptions of my other field sites' in terms

of setting and methods are available in the appendices, but the breadth of each site's data description is dependent on whether ^{10}Be concentrations have been measured for that site's samples. These sections for my field sites besides the Great Smoky Mountains are meant to be preparation for a longer paper for submission to a peer-reviewed journal that will include all my data when they are available. The thesis will then conclude with a brief summary of what has been learned from this experiment, and with recommendations about how best to apply these methods in the future. Specifics on soil pits, field observations, ^{10}Be concentrations, and GPS locations for samples are contained in appendices.

CHAPTER 2: LITERATURE REVIEW

The processes that shape landscapes are of fundamental importance to geomorphologists. These processes act on the scale of mountain ranges, drainage basins, hillslopes, and soil profiles. Geomorphologists have gained a better understanding of erosional processes and patterns for mountain ranges, drainage basins, and outcrops through the measurement of cosmogenic nuclides, a technique developed over the last two decades (Gosse and Phillips, 2001; Lal, 1991). Much less cosmogenic research has focused on hillslope-scale sediment production and transport (Heimsath et al., 1997, 1999; Heimsath, 2005). Recently, there has been a call for just the type of field-based investigations of hillslope processes that cosmogenic analysis of hillslope soils would provide (Dietrich, 2003). The quantification of the rates soil production and transport on hillslopes contributes to the understanding of hillslope behavior directly as well as contributing to the discussion of basin-scale landscape evolution where hillslope processes are often cited as important, but are rarely addressed in a quantitative manner (Bierman and Steig, 1996; Brown et al., 1995; Matmon et al., 2003b).

2.1 Cosmogenic Nuclides

Cosmic ray bombardment of the Earth creates ^{10}Be in the first few meters below the surface (Lal and Peters, 1967). The near-surface exposure history of a bedrock surface or grain of sediment can be determined by measuring ^{10}Be concentrations in

quartz (Bierman and Steig, 1996; Lal, 1991). The near-surface residence time represented by the ^{10}Be concentration depends on erosion rate. For rapidly eroding sites, the time over which ^{10}Be is being produced might only be millennia (Duncan et al., 2001) and resulting ^{10}Be concentrations are very low, 10^4 atoms per gram. For very stable sites, such as hyper-arid passive margins (Bierman and Caffee, 2002) and Antarctica (Nishiizumi et al., 1991), production times may approach a million or more years resulting in extremely high ^{10}Be concentrations on the order of 10^6 to 10^7 atoms per gram. The application of *in situ* produced cosmogenic radionuclides to quantify the rate of sediment generation and transport on steep hillslopes is a relatively new use for this isotopic technique (Heimsath et al., 2002; Heimsath et al., 2001). Heimsath et al. used ^{10}Be abundances in hillslope sediment to model the maintenance of a soil mantle through a balance between sediment production and hillslope erosion. This work did not track nuclide abundances as a function of movement downslope away from loci of sediment production. In contrast, Nichols et al., (2002) quantified sediment transport on moderately to shallowly sloping (~2^o) desert piedmonts in the eastern Mojave Desert but did not consider sediment production from bedrock. They were able to demonstrate that sediment is uniformly dosed by cosmic rays as it is transported away from the mountain fronts based on observations of a roughly linear relationship between distance from rangefront and nuclide concentration in piedmont sediment.

Sediment production and transport on steep hillslopes have been examined quantitatively using atmospherically produced ^{10}Be (McKean et al., 1993). Atmospheric ^{10}Be refers to nuclides produced in the atmosphere by nuclear reactions, deposited by

rainfall, and adhered to soil grains, as opposed to the ^{10}Be created within soil grains (*in situ*) that I measured. These two types of ^{10}Be are separated in the lab by repeated acid etching of quartz grains to remove any surface-adhered ^{10}Be (Brown et al., 1991; Gosse and Phillips, 2001; Nishiizumi et al., 1991). If this atmospheric ^{10}Be were not removed, it would overwhelm our attempt to measure *in situ*-produced ^{10}Be. The rate at which sediment is produced from rock is key to understanding how soil mantles are maintained over a wide range of erosional, tectonic, lithologic, and climatic settings (Heimsath et al., 2002; Heimsath et al., 1997; Heimsath, 2005). Because cosmogenic radionuclides such as ^{10}Be can be used to constrain rates of sediment production (Heimsath et al., 2001; Heimsath, 2005) and trace transport down slope and into channel systems (Nichols et al., 2002), cosmogenic analyses are now often used to supplement and/or support previous work based on more traditional geomorphic techniques. For example, sediment yield estimates suggest that the Oregon Coast Range is in equilibrium as regards soil production driven by rock weathering and soil loss due to tectonically and climatically driven erosion (Reneau and Dietrich, 1991). Heimsath et al., (2001), Bierman et al., (1998), and Bierman et al., (2001) used the cosmogenic nuclides ^{10}Be and ^{26}Al to estimate basin-scale erosion rates in the Oregon Coast Range so they could test the assumption (by comparision with sediment yield) that this is indeed an equilibrium landscape. Their cosmogenically-deduced conclusions supported Reneau and Dietrich's earlier assertion that the landscape was in equilibrium and allowed a clearer understanding of the spatial distribution of slope processes leading to that equilibrium.

Recently, cosmogenic radionuclides have been used in conjunction with other techniques, such as sediment budgeting and fission track dating, to provide a more complete picture of landscape evolution (Kirchner et al., 2001; Matmon et al., 2003a; Matmon et al., 2003b; Nichols et al. 2005). For example, in the Great Smoky Mountains of the southern Appalachians, Matmon et al. found that late Cenozoic erosion rates calculated from cosmogenic nuclide concentrations agreed well with longer-term exhumation rates determined from fission tracks and contemporary erosion rates deduced from modern sediment budgets. In contrast, Kirchner et al.'s controversial work in the Idaho batholith found that erosion rates measured with cosmogenic nuclides agreed well with rates from fission tracks, but were 17 times higher than rates measured through decadal scale budgets of sediment fluxes. It is possible that an understanding of erosion speed and locale on the slopes could help resolve these conflicts between basin-scale data integrating over different time frames.

2.2 Soil Transport Laws

Gravity-driven soil diffusive processes, such as soil creep, have long been considered important for sediment transport during the evolution of soil-mantled landscapes. Early observational studies defined a proportional link between hillslope gradient and rate of soils' downslope transport, with those components eventually reaching dynamic equilibrium (Gilbert 1877, 1909). Gilbert assumed a uniform soil thickness and a uniform rate of soil production, requiring soil velocity to increase with distance from the top of the slope in order to "keep up" with soil flux. Consequently, a

slope's gradient must increase linearly downslope – creating a convex upward profile – to provide the necessary transport capacity (Gilbert, 1909). This inferred linear relationship between gradient and soil transport has been the basis for many soil-transport laws and hillslope evolution models (e.g., Carson and Kirkby, 1972). The simplest of these soil-transport laws state that sediment flux, q_s, is proportional to gradient, ∇z, such that $q_s = -K\nabla z$; here K is equivalent to a diffusion coefficient with dimensions $(\text{length})^2 (\text{time})^{-1}$ (Martin, 1997). A criticism of these laws that assume linear diffusivity is that their appeal, and geomorphologists' reliance on them, is the result of their mathematical simplicity rather than any process-based confirmation (Heimsath, 2005).

However, not all models for hillslope transport rely on the assumption of linear diffusivity, and nonlinear diffusion has been especially successful in describing soil transport on steep slopes (Andrews, 1975; Martin, 1997; Roering, 2001a, b; Roering, 2005). Efforts to define a transport law for nonlinear diffusion have relied largely on experimental modeling with little emphasis on direct measurements of processes in the field. For example, Roering (2001b) created an experimental hillslope using sand-sized grains that were disturbed using random acoustic noise. This study found that soil transport rates increased nonlinearly with respect to gradient as a critical slope, S_c, was approached

$$\bar{q}_s = \frac{K\nabla z}{1 - (|\nabla z|/S_c)^2} \qquad (1)$$

where q_s is soil flux, $\nabla z = \tan\theta$, and K is a diffusivity constant. In a natural setting, surpassing S_c would equate with steepening a hillslope's gradient such that its soil

mantle's shear strength has been overcome. In these nonlinear models, a hillslope's profile is convex close to the hillcrest, but becomes planar downslope as it approaches S_c (Roering, 2001a). It follows, then, that in landscapes where diffusion is nonlinearly related to hillslope gradient, hillslope relief and slope angle are not sensitive indicators of erosion rate (Roering, 2001a). This final point is especially important when considering hillslope form as an indicator of larger-scale landscape evolution. If a landscape's soil diffusion is nonlinear, then the average gradient of hillslopes cannot be used to infer whether an area has achieved an equilibrium between soil production and erosion.

Steep hillslopes in the Oregon Coast Range are a good example of an environment in which nonlinear diffusion models are especially applicable. The analysis of hillslope morphology pre- and post-fire events has supported nonlinear diffusion models using a blend of high-resolution topographic surveying and modeling (Roering and Gerber, 2005). Speaking in terms of the nonlinear model presented above, these researchers found hillslopes' post-fire S_c to be lower than that of the pre-fire landscape. The result was post-fire soil fluxes that were six-fold higher than long-term average rates. The use of Airborne Laser Swath Mapping (ALSM) in this study allowed the authors to create very high-resolution topographic models for soil diffusion on pre- and post-fire hillslopes. Measurements of dry ravel transport on the post-fire hillslopes helped calibrate the models, but these modeled rates still relied heavily on assumptions inherent in the nonlinear diffusion model. All current models of hillslope processes would benefit from more rigorous efforts to calibrate transport rates based on field measurements.

Most diffusion models, both linear and nonlinear, are contingent upon the modeled landscape being in steady-state (Davis, 1892; Gilbert, 1909; Heimsath et al., 1997; Monaghan, 1992; Roering, 2001a; Small et al., 1999; Willet, 2002). For this assumption to hold true, soil production on a hillslope must be balanced by soil flux (Willet and Brandon, 2002). This balance is most commonly achieved in models by assuming the thickness of the soil mantle is constant through time, thus downslope soil velocities, and by extension soil fluxes, increase to keep pace with soil production and the transport of soil from upslope positions. So, if the rate of soil production on a hillslope can be determined, then soil volume flux can also be calculated. When considered in conjunction with the tangent of local slope angles, these calculated soil fluxes can yield diffusion coefficients, *K* from above, for a given environment. There are several good examples of this approach to quantifying diffusion coefficients.

McKean et al., (1993) use meteoric ^{10}Be to investigate soil production rates of clay soils in Contra Costa County, CA. By adapting the methods of (Monaghan, 1992), these researchers calculate soil production rates of 0.026 ± 0.007 $cm \cdot yr^{-1}$ and associated soil flux rates of 0-82 $cm^3 \cdot yr^{-1} \cdot cm^{-1}$. The tangent of the slope angle for the study's hillslope ranges from 0-0.22, and soil flux rate increases proportionally to hillslope gradient. The average diffusion coefficient for this site is 360 $cm^3 \cdot yr^{-1} \cdot cm^{-1}$, and a linear increase in creep flux with soil gradient cannot be rejected. Small et al., (1999) obtain similar results based on rates of regolith production on a convex alpine hillslope in the Wind River Range, WY. They find that regolith is being produced at a rate of 0.0143 ± 0.004 $cm \cdot yr^{-1}$ and that flux rates range from 0-22 $cm^3 \cdot yr^{-1} \cdot cm^{-1}$. The tangent of slope

angle for this convex slope ranges from 0-0.15, and the average diffusion coefficient is 182 ± 20 $cm^3 \cdot yr^{-1} \cdot cm^{-1}$. The authors conclude that not only is this slope in steady-state, but, based on the age of adjacent summit flats, these conditions have been achieved in less than several million years.

Analysis of *in situ*-produced ^{10}Be has proven itself as a robust method for quantifying rates of soil production under varying levels of soil cover (Heimsath et al., 1997, 1999; Small et al., 1999). Recently, Heimsath et al. (2005) combined comprehensive surveying of hillslopes' soil mantle thickness with equally comprehensive calculations of soil production rates derived from ^{10}Be concentrations at the soil-bedrock contact. These researchers found that a linear diffusion law did not adequately describe the patterns of soil flux modeled from their soil production rates. Instead, they found soil transport to be a nonlinearly related to soil mantle thickness with an exponential decline in soil production with increasing soil thickness. These results do not rule out linear diffusion on low-gradient convex hillslopes, or sections of hillslopes adjacent to a hillcrest. However, this work is further evidence that careful field-based observations and measurements of hillslope morphology can lead to more widely applicable transport laws for hillslope processes.

CHAPTER 3: METHODS

Sample collection methods we describe below rely on both natural (soil mixing) and field amalgamation (mixing samples from soil pits) techniques. The approach is modified from the low-gradient desert piedmont sampling methods of Nichols et al. (2002) for use on much steeper and shorter hillslopes in more humid climate zones. At each site, we collected and mixed samples from numerous soil pits as described below amalgamating and homogenizing samples collected on contour-parallel transects.

3.1 Site Selection

We selected hillslopes for sampling in areas where previous work provided context for our own results. Selected sites are located in different tectonic and climatic settings including active and passive margins and temperate and humid climatic regimes. We did this so that our results would provide testable hypotheses regarding the influence of climate and tectonics on hillslope process rates.

After selecting regions to investigate, we used topographic and geologic maps to select hillslopes to sample. Ideal slopes for sampling are planar and large enough to allow ridge-parallel transects that are at least 300 m-long, and at least a 50 m downslope distance between each transect. Site accessibility to roads and trails was also important since the amount of soil sampled (>5 kg per sample) is large enough that carrying it by foot over long distances is not practical. We selected hillslopes on quartz-bearing lithologies of a to allow measurement of in situ as well as meteoric ^{10}Be concentrations.

3.2 Field Methods

After an area had been selected for sampling, we did fieldwork to verify the planar slope morphology suggested by the topographic maps and to select specific sample collection sites. We dug several test pits to understand soil texture, structure, and horizon development. This information allowed us to design a specific sampling protocol for each slope including distance from the ridgeline to the first sampling transect, transect length, soil pit spacing along each transect, transect to transect spacing, and sampling depths within each soil pit.

The sampling techniques used on each hillslope were the same. The first transect was located a short distance downslope from the ridgeline and the first pit was excavated creating one endpoint of the topmost transect. Samples are collected from several depths within this and all other pits as determined by evaluations of soil morphology and development during reconnaissance. For example, along each transect and from each pit, in the Great Smoky Mountains, equal volumes of soil were collected from the A-horizon, the top of the B-horizon, and the bottom of the B-horizon. Samples from each horizon were amalgamated separately.

During sampling, soil descriptions were made for each pit including depths of horizons, horizon colors, soil textures, and structure. Each soil pit was located using a Garmin 75 GPS unit. In the Great Smoky Mountains, a Trimble ProXH was used to provide post-processed location data with decimeter precision. For each of our hillslopes,

we sampled a total of seven pits along each transect. We collected, and analyzed separately, samples from four distinct transects (Figure 1).

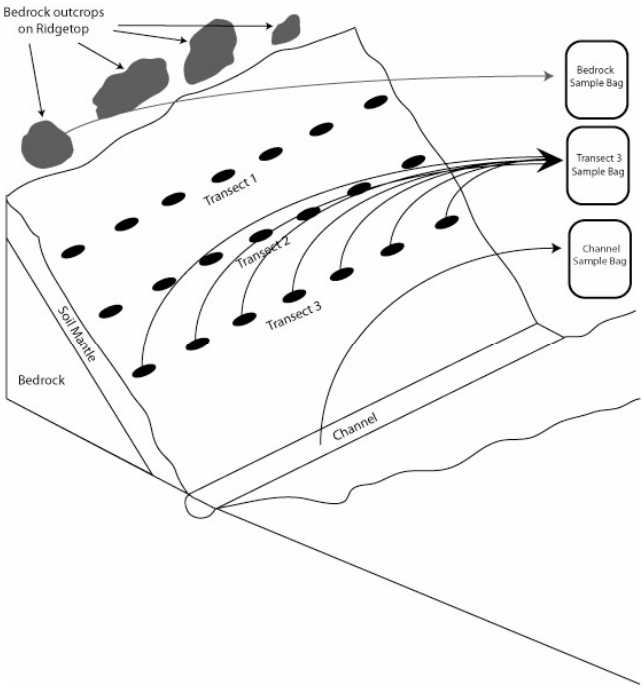

Figure 1. Schematic of hillslope sampling technique. Samples are collected from pits dug along hillslope transects and combined into amalgamated samples, one per transect. Discrete bedrock samples are collected along the ridgetop as potential sediment production loci. Channel sediment samples confirm basin-scale erosion rates and provide context for the hillslope data based on sediment from upstream hillslopes.

In the Great Smoky mountains, we kept samples from the seven pits along one transect separate in order to understand the spatial variability of nuclide concentrations pit to pit. In the Smoky Mountain site we also drove a two-meter metal rod to refusal adjacent to each pit in order to determine how the soil-bedrock contact depth changed both downslope and across slope.

At some sites, we collected samples from other portions of the hillslope. Where bedrock cropped out on hilltop ridges, we sampled such outcrops to determine a lowering

rate for the ridgeline. We also collected sediment from streams adjacent to sampled hillslopes so that we can measure an erosion rate for the basin within which the hillslopes were contained. In the Great Smoky Mountains, NC, and the Drift Creek Wilderness, OR, we collected samples from small valleys that bounded one end of the hillslope. These samples provide an isotopic concentration for sediment being transported from the sampled hillslope before it enters the bounding stream downslope.

3.3 Laboratory Methods

We prepared samples for analysis of *in situ*-produced ^{10}Be. First, samples were wet-sieved to remove material <125μm in diameter. Samples were then dried, and then sieved to isolate the 250-850 μm fraction from which quartz was extracted. Bedrock sample and clasts were crushed, ground, and sieved. Quartz was purified by standard procedures (Kohl and Nishiizumi, 1992) with the HCl etch step repeated several times for many samples, usually for samples from shallow soil horizons.

CHAPTER 4: *GEOLOGY* PAPER

Deciphering Diffusion: *In situ*-produced ^{10}Be as a Geomorphic Tracer of Hillslope Sediment Production and Transport

March, 2007

Matthew C. Jungers
Department of Geology, University of Vermont, Burlington, VT, 05405, USA

Paul R. Bierman
Department of Geology and School of Natural Resources, University of Vermont, Burlington, VT, 05405, USA

Ari Matmon
Institute of Earth Sciences, Hebrew University, Givat Ram, Jerusalem, 91904, Israel

Kyle Nichols
Department of Geosciences, Skidmore College, Saratoga Springs, NY, 12866, USA

Jennifer Larsen
Department of Geology, University of Vermont, Burlington, VT, 05405, USA

Robert Finkel
Center for Accelerator Mass Spectrometry, Lawrence Livermore National Laboratory, Livermore, California, 94551, USA

Keywords: geomorphology, Great Smoky Mountains, hillslope, soil transport, cosmogenic nuclides

ABSTRACT

A simple, widely applicable technique for directly measuring both soil production and transport on geologically meaningful timescales is lacking. Here, we use *in situ*-produced, cosmogenic ^{10}Be as a tracer of soil production and transport in the Great Smoky Mountains, NC. Our work relies upon the power of amalgamation to both investigate and to smooth spatial variance in ^{10}Be concentrations. Using cosmogenically produced isotopes as a geomorphic tracer allows us to both quantify soil production and track soil as it is transported downslope. Best-fit models of the data require soil velocities of 1-3 $cm \cdot yr^{-1}$ in the well-mixed active layer of the soil. The thickness of this active transport layer is dependent on the rooting depth of trees on the slope and the related depth of soil turnover and mixing due to treethrow. Modeled soil fluxes range from 55-165 $cm^3 \cdot yr^{-1} \cdot cm^{-1}$ depending on whether soil velocity or the thickness of the actively transported layer is kept constant downslope. Diffusion coefficients calculated from these flux rates range from 82-247 $cm^3 \cdot yr^{-1} \cdot cm^{-1}$. This range of diffusion coefficients on our slope may be accounted for by either a transition to nonlinear diffusion below the hillcrest, or a climate-driven change in floral assemblage on the slope that provided a deeper effective rooting depth. Deeper roots would increase the mixing depth for actively transported soil. This hillslope does not appear to be in steady state, calling into question what constitutes a state of steady erosion for an ancient mountain range such as the Appalachians.

INTRODUCTION

Understanding where and how quickly soil is produced and transported has important implications for land management, agriculture, and understanding the pace and process of landform development (Heimsath, 2005; Wells, 1993; Willet, 2002). However, a simple, universally applicable technique for directly measuring both soil production and transport on geologically meaningful timescales is lacking.

The two most important components of any model for hillslope sediment transport are 1) the rate at which soil is being produced from underlying bedrock, and 2) the flux of soil downslope from the hillcrest (Carson, 1972). These two parameters are intimately linked, with soil production being greater than flux on an erosion-limited slope, and soil flux outstripping production on a weathering-limited slope. A hillslope in steady-state has soil production balanced by soil flux (Willet, 2002). The question of how such a balance might be achieved has long challenged geologists (Davis, 1892; Gilbert, 1877). Early models for equilibrium hillslopes required a directly proportional relationship between soil flux and topographic gradient (Davis, 1899; Gilbert, 1877, 1909; Penck, 1953). Under such conditions, a hillslope was posited to develop a convex profile, thus increasing gradient in order to balance the increasing flux of soil downslope. These early models are still the starting point for most current models of hillslope soil transport (Heimsath, 2005; McKean et al., 1993; Roering, 1999).

Recent advances in understanding of hillslope processes may be grouped into two general categories: 1) studies that use precise topographic measurements or experimental

data to explore how soil flux and gradient are linked (Roering, 2001a, b; Roering, 2005) and 2) studies that quantify soil production and use those rates to estimate soil flux under steady-state conditions (McKean et al., 1993; Monaghan, 1992; Small et al., 1999). Some studies combine measurements of soil production with topographic data (Heimsath et al., 1999, 2001; Heimsath, 2005; Roering, 2002). Recently, there has been a call for more field-based investigations of hillslope processes (Dietrich, 2003; Heimsath, 2005) in the hope that models will develop that are unconstrained by conventional assumptions of linear diffusivity. Such models would be further enriched if they were able to quantify hillslope sediment production and transport on timescales that are geologically (centuries to millennia) relevant (Fleming, 1975; Heimsath, 2005; McKean et al., 1993; Small et al., 1999).

Here, we use *in situ*-produced, cosmogenic ^{10}Be to trace soil production and transport in forested, mountainous terrain. Our work relies upon the power of amalgamation to both investigate and smooth spatial variance in ^{10}Be concentrations (Bierman et al., 2006). Using cosmogenically produced isotopes as a geomorphic tracer not only allows us to quantify soil production (Heimsath et al., 1997), but also to track soil as it is transported downslope. The location of the sample site within an ancient mountain range, the Appalachians, provides the context to consider hypotheses about how soil flux relates to landscape equilibrium and orogen evolution.

SETTING

The field site is located within a soil-mantled upland basin of the Great Smoky Mountains, NC, where rates of hillslope soil transport are erosion-limited (Figure 1). This is a landscape for which erosion rates have been quantified and steady erosion over time has been suggested (Matmon et al., 2003a; Matmon et al., 2003b). We sampled a planar hillslope (15^{o}) with a maximum elevation of 1606 m, and a local relief of 98 m between the hillcrest and Flat Creek, which is the lower boundary of the slope. The distance from the ridge to Flat Creek is approximately 400 m. The entire hillslope is underlain by quartz-rich, metamorphosed conglomeratic sandstone (Thunderhead Formation). Bedrock outcroppings are limited to the hillcrest and the floors of draws that incise the slope's soil mantle. Mean annual precipitation in the Great Smoky Mountains ranges from 1.4 to 2.3 m, with higher values corresponding to higher elevations such as the field site (http://www.nps.gov/grsm/gsmsite/natureinfo.html; accessed January 2007).

The slope is well vegetated. Deciduous trees such as American beech (*Fagus grandifolia*) dominate a discontinuous forest canopy. The forest has been disturbed by tree throws, especially near the hillcrest. Low-lying shrubs and briars fill canopy openings created by tree falls. It appears that the dominant mechanism for biogenic soil transport on this hillslope is tree throw associated with the uprooting of mature trees by wind (Figure 2). We posit that this tree throw creates an active transport layer (Lekach, 1998) approximately 55 cm thick. Within this layer, soil is well-mixed and transported at a constant velocity, yielding a velocity profile analogous to curve "B" in Figure 2.

METHODS

Our sampling strategy relied on the mixing of soil to average unique grain histories for cosmogenic analysis. Some mixing is natural (bioturbation), while other mixing we did by amalgamating subsamples from different soil pits across hillcrest-parallel transects. Our approach is adapted from low-gradient, desert piedmont sampling methods (Nichols et al., 2002) for use on this steeper and shorter.

Samples were collected along four hillcrest-parallel, 300 meter-long transects set at equal distances downslope (Figure 3a). Along each transect, seven soil pits were excavated at 50 m intervals and equal volumes of soil were collected from each pit at depths of 10-15 cm, 30-35 cm, and 50-55 cm. Clasts were collected at the top of the soil-saprolite boundary (60 cm depth). Samples from each depth were amalgamated separately. At each pit, we noted soil horizonation and drove a 2-m metal rod to refusal. Along the second transect downslope (MJGS3A-G or T2), we kept samples from the seven pits separate in order to understand the spatial variability of nuclide concentrations pit to pit. We took a sediment sample from a small draw along the southern boundary of the slope so that we knew the ^{10}Be concentration of sediment being transported from the sampled hillslope into the bounding stream downslope.

Beryllium was extracted from 13 to 41 g quartz. Samples were processed at the University of Vermont using standard techniques and analyzed at Lawrence Livermore National Laboratory. A blank was processed with each batch of 7 samples. The resulting blank correction was at most several percent of sample ^{10}Be/^{9}Be ratios. We developed simple mass balance models incorporating ^{10}Be concentrations, soil production rates

(Heimsath et al., 1997), and field observations to consider rates of soil transport downslope (Data Repository).

DATA

Quartz from the Great Smoky Mountains contains significant amounts of ^{10}Be (4.1 to 7.2 x 10^5 atoms g^{-1}, Data Repository Table 1). Concentrations of ^{10}Be in amalgamated transect soil samples increase linearly between transects 1 (MJGS2), 2 (MJGS3A-G) and 3 (MJGS4), but a systematic drop in ^{10}Be concentrations occurs (squares, circles, triangles) at transect 4 (MJGS5). Concentrations for clasts (diamonds) increase linearly downslope from transect 1-4 (Figure 3b). Fluvial sediment from a draw along the southern boundary of the hillslope (MJGS6) has the highest ^{10}Be concentration, 7.2 x 10^5 atoms g^{-1}.

Along transect two (T2), there is significant variability between pits (samples MJGS3A-G) both in ^{10}Be concentration and in the relationship of ^{10}Be concentration to depth. From pit to pit, there is no consistent increase or decrease in ^{10}Be concentration with respect to sample depth (Figure 4a). However, the range of ^{10}Be concentrations does increase with both sample depth and grain size; standard deviation as percentage of the mean increases from 11% (10-15 cm depth) and 10% (30-35 cm depth) to 16% at 50-55 cm depth and 26% for clasts at 60 cm depth. Amalgamated samples from T1, T3, and T4 also lack a significant relationship between ^{10}Be concentration and depth. Concentrations for soil samples (from depths of 10 cm, 30 cm, and 50 cm) along T1 and

T3 are indistinguishable within analytical error for each transect (Figure 4b), implying the soils we sampled are well-stirred. Only on T4 does soil from a depth of 60 cm have a significantly lower ^{10}Be concentration than shallower samples, 4.9 x 10^5 atoms g^{-1}.

Based on a simple mass balance model incorporating both soil mass and cosmogenic ^{10}Be abundance, ^{10}Be concentrations measured in the Great Smoky Mountains can be achieved by 1) increasing downslope soil velocity from 1 cm·yr^{-1} at the top transect to 3 cm·yr^{-1} at the final transect with a constant active layer thickness of 55 cm, or 2) allowing the thickness of the active layer to increase downslope by a maximum of 30 cm resulting in an active layer that thickens from 55 cm at the top of the slope to 85 cm by the bottom transect while keeping soil velocity constant at 1 cm·yr^{-1}. Field data cannot help us resolve which of these scenarios is more reasonable.

DISCUSSION

By physically mixing samples to smooth the idiosyncratic histories of individual grains, and by measuring cosmogenic ^{10}Be abundances in those grains, we are able to consider hillslope processes on geologically meaningful spatial and temporal scales. Using ^{10}Be as a geomorphic tracer, we do not rely on any assumed proportional relationship between soil production/transport and hillslope gradient; rather, our interpretation is constrained by measured nuclide concentrations and the conservation of mass which mandates that soil flux increases downslope as soil is both produced from underlying bedrock and transported from upslope positions.

Best-fit models of the cosmogenic data require soil velocities of 1-3 $cm \cdot yr^{-1}$ in the well-mixed active layer of the soil. Associated soil fluxes range from 55-165 $cm^3 \cdot yr^{-1} \cdot cm^{-1}$, depending on whether soil velocity or the threshold depth for the active transport layer is kept constant. Since our slope is planar, any calculations of diffusion coefficients require a nonlinear relationship between hillslope gradient and flux (Roering, 1999). If we assume that this hillslope's gradient of 0.27 is *approaching* a critical hillslope gradient (S_c) as required by the model cited above, then by setting S_c at 0.35, a value considerably higher than our hillslope's gradient, we calculate diffusion coefficients of 82-247 $cm^3 \cdot yr^{-1} \cdot cm^{-1}$.

The soil velocities and associated soil fluxes that our data suggest are consistent with rates measured by different means on hillslopes in other environments (Heimsath, 2005; McKean et al., 1993; Roering, 2002; Small et al., 1999). McKean et al., (1993) measured fluxes of 65-111 $cm^3 \cdot yr^{-1} \cdot cm^{-1}$ for clay-rich, grass-covered soils on low-gradient slopes (0-0.22) east of San Francisco, CA; the corresponding diffusion coefficients for this weak soil are 360 ± 55 $cm^3 \cdot yr^{-1} \cdot cm^{-1}$. A better comparison for soil conditions at our site are the more competent, coarse-grained forested hillslopes of the Oregon Coast Range. However, soil flux in the Great Smoky Mountains is notably higher than these slopes, which have fluxes of 32 ± 23 $cm^3 \cdot yr^{-1} \cdot cm^{-1}$ and associated diffusion coefficients of 48 ± 34 $cm^3 \cdot yr^{-1} \cdot cm^{-1}$ (Reneau and Dietrich, 1991). Lower values of 0-22 $cm^3 \cdot yr^{-1} \cdot cm^{-1}$ and 182 ± 20 $cm^3 \cdot yr^{-1} \cdot cm^{-1}$ for soil flux and diffusivity, respectively, have been reported for sediment transport on lower gradient slopes (maximum gradient = ~7°) in an alpine setting (Small et al., 1999).

Unlike the studies cited above, our data do not allow us to evaluate a linearly proportional relationship between soil flux and hillslope gradient. This may be attributed to both experimental design and biogenic factors. The proportional relationship between soil flux and hillslope gradient is most readily observed near a hilllslope's low gradient, convex hillcrest (McKean et al., 1993; Roering, 1999; Small et al., 1999). Since we purposely located transects on the slope's planar surface below the hillcrest, it is possible that transport had transitioned from linear diffusion to nonlinear diffusion before our first transect. Such a transition would require that the average slope angle of ~15^{o} in the Great Smoky Mountains must approximate, or be approaching, S_c for this site, such that the soil's shear strength has been surpassed, and soil flux may increase without a steepening of the slope (Roering, 1999). The potential of accommodating increased soil flux downslope by thickening the actively transported layer of soil, rather than increasing hillslope gradient, could be achieved by a change in floral assemblage over the timescale that ^{10}Be accumulates in the soil (Roering, 2002). If the slope was vegetated by larger trees with a deeper rooting depth during pre-settlement times, the active transport layer may have been thicker than our modern observations suggest. This is especially likely low on the slope where trees are more sheltered from high wind events. This biogenic influence on soil flux would mean that climate-driven changes in vegetation could be a strong factor controlling soil transport rates independent of slope gradient on a geologic timescale (Roering, 2002).

None of our best-fit models were able to account for the drop in the soil ^{10}Be concentrations for the final transect. This drop in ^{10}Be abundance could be accounted for

in two ways. If non-diffusive convergence into fluvial draws causes more soil transport low on the slope, then surface soil along T4 may be stripped to a depth where isotope concentrations are weighted toward the ^{10}Be activity of the underlying saprolite (Figure 3b). It is also possible that this hillslope is in a transient phase from a period of higher flux rates during periglacial conditions of the last full glacial period approximately 12,000-30,000 years ago. If this were the case, the isotopic signature of the bottom transect would be the trailing end of a plug of "glacial" soil being moved off the slope at slower modern rates. Such a disparity between modern, non-periglacial rates and rates during the last glacial maximum is consistent with compilations of erosion rate data (Young, 1960).

The complex relationship between soil thickness, downslope flux of soil, and hillslope gradient in the Great Smoky Mountains suggests a transient landscape rather than one in steady state. This calls into question not only conventional steady-state assumptions in other models for hillslope processes, but also our perception of what to expect in an "old" mountain range such as the Appalachians. Our results show that on the scale of a hillslope, cycles of climate change much shorter than the age of a mountain range could cause perturbations in soil flux rates that might not be expected for landscapes assumed to be eroding steadily. Expansion of our field and lab methods to other environments, and more thorough consideration of this hillslope's topography are the next steps in deciphering complex feedbacks between climate, hillslope gradient, soil transport rates, and time.

ACKNOWLEDGEMENTS

Paper benefited from conversations with A. Heimsath and J. Roering. Field work, sample analysis, and research were supported by NSF (EAR-310208), USGS (04ERAG0064), and DoD (DAAD19-03-1-0205).

Figures Captions

1. Location map with the Great Smoky Mountains (GSM), denoted within inset map of eastern United States, North America. Sampled area is marked by a small trapezoid on topographic base map, USGS *Bunches Bald* quadrangle, UTM Zone 17, NAD 83 Datum.

2. Soil transport on sampled hillslope is driven by tree throw associated with uprooting of mature trees. (a) Fresh rootwad with P. Bierman (1.8 m) as scale. Rootwads such as this commonly overturn soil up to a depth of 55-60 cm. Weathered clasts such as we sampled at the base of soil pits are visible on the base of the rootwad. (b) Schematic showing how tree throw events can create a threshold depth for soil velocity profiles in disturbance-dominated environments (inset graph adapted from Roering et al., 2002). Over time, soil is thoroughly mixed in an active layer with a thickness equal to this threshold depth.

3. Sampling schematic and downslope patterns of measured ^{10}Be. (a) Samples are grouped in boxes, and for each box four different sample types were collected: 1) soil A-horizon from 10-15 cm, 2) soil upper B-horizon from 30-35 cm, 3) soil lower B-horizon from 50-55 cm, and 4) clasts from the soil-saprolite boundary at ~60 cm. (b) Concentrations of ^{10}Be in amalgamated transect soil samples increase linearly between transects 1, 2 and 3, but a systematic drop in ^{10}Be concentrations occurs (squares, circles, crosses) at transect 4. Concentrations for clasts (triangles) increase linearly downslope from transect 1-4. Samples' distances downslope are offset for clarity. Error bars represent 1σ analytical error for T1, T3, and T4. On T2, error bars are 1 standard error of the mean (n=7).

4. Patterns of measured ^{10}Be concentrations vs. sample depth. (a) ^{10}Be concentrations for individual pits along T2. The range of concentrations in soil samples increases with depth suggesting a threshold depth of 30-50 cm for mixing efficiency. The largest range of concentrations is for saprolite clasts at 60 cm. Error bars represent analytical error. (b) ^{10}Be concentrations vs. sample depth for each transect. Concentrations for soil samples are similar within error for T1-T3, suggesting soil is well mixed to a depth of 55 cm for most of the hillslope. There is no consistent relationship between ^{10}Be concentrations and depth for saprolite clasts at 60 cm. Error bars represent 1σ analytical error for T1, T3, and T4. Error bars for T2 are 1 standard error of the mean (n=7). (c) Photograph of a representative soil pit and a schematic of soil horizons.

REFERENCES CITED

Carson, M.A., Kirkby, M.J., 1972, Hillslope form and process: Cambridge University Press, New York, p. 475.

Davis, W.M., 1892, The convex profile of badland divides: Science, v. 20, p. 245.

—, 1899, The Geographical Cycle: The Geographical Journal, v. 14, p. 481-504.

Dietrich, W.E., Bellugi, D., Heimsath, A.M., Roering, J.J., Sklar, L., and Stock, J.D., 2003, Geomorphic transport laws for predicting landscape form and dynamics, in Wilcock, P., and Iverson, R., eds., Prediction in Geomorphology, Volume Geophysical Monograph 135: Washington, D.C., American Geophysical Union, p. 103-132.

Fleming, R.W., and Johnson, A.M., 1975, Rates of seasonal creep of silty clay soil: Q.J. Engineering Geology, v. 8, p. 1-29.

Gilbert, G.K., 1877, Geology of the Henry Mountains (Utah): US Geographical and Geological Survey of the Rocky Mountains Region, 160 pp.

—, 1909, The convexity of hilltops: Journal of Geology, v. 17, p. 344-350.

Heimsath, A.M., Dietrich, W.E., Nishiizumi, K., and Finkel, R.C., 1997, The soil production function and landscape equilibrium: Nature (London), v. 388, p. 358-361.

—, 1999, Cosmogenic nuclides, topography, and the spatial variation of soil depth: Geomorphology, v. 27, p. 151-172.

—, 2001, Stochastic processes of soil production and transport; erosion rates, topographic variation and cosmogenic nuclides in the Oregon Coast Range: Earth Surface Processes and Landforms, v. 26, p. 531-552.

Heimsath, A.M., Furbish, D.J., and Dietrich, W.E., 2005, The illusion of diffusion: Field evidence for depth-dependent sediment transport: Geology, v. 33, p. 949-952.

Lekach, J., Amit, R., Grodek, T., Schick, A.P., 1998, Fluvio-pedogenic processes in an ephemeral stream channel, Nahal Yael, Southern Negev, Israel.: Geomorphology, v. 23, p. 353-369.

Matmon, A., Bierman, P.R., Larsen, J., Southworth, S., Pavich, M., and Caffee, M., 2003a, Temporally and spatially uniform rates of erosion in the southern Appalachian Great Smoky Mountains: Geology, v. 31, p. 155–158.

Matmon, A.S., Bierman, P., Larsen, J., Southworth, S., Pavich, M., Finkel, R., and Caffee, M., 2003b, Erosion of an ancient mountain range, the Great Smoky Mountains, North Carolina and Tennessee: American Journal of Science, v. 303, p. 817-855.

McKean, J.A., Dietrich, W.E., Finkel, R.C., Southon, J.R., and Caffee, M.W., 1993, Quantification of soil production and downslope creep rates from cosmogenic 10Be accumulations on a hillslope profile: Geology, v. 21, p. 343-346.

Monaghan, M.C., McKean, J., Dietrich, W., and Klein, J., 1992, 10-Be chronometry of bedrock-to-soil conversion rates: Earth and Planetary Science Letters, v. 111, p. 483-492.

Nichols, K.K., Bierman, P.R., Hooke, R.L., Clapp, E., and Caffee, M., 2002, Quantifying sediment transport on desert piedmonts using ^{10}Be and ^{26}Al: Geomorphology, v. 45, p. 89-104.

Penck, W., 1953, Morphological analysis of landforms: London, MacMillian, p. 429.

Reneau, S.L., and Dietrich, W.E., 1991, Erosion rates in the southern Oregon Coast Range: evidence for an equilibrium between hillslope erosion and sediment yield: Earth Surface Processes and Landforms, v. 16, p. 307-322.

Roering, J.J., Almond, P., Tonkin, P., and McKean, J., 2002, Soil transport driven by biological processes over millennial time scales: Geology, v. 30, p. 1115-1118.

Roering, J.J., Kirchner, J.W., and Dietrich, W.E., 1999, Evidence for nonlinear, diffusive sediment transport on hillslopes and implications for landscape morphology: Water Resources Research, v. 35, p. 853-870.

—, 2001a, Hillslope evolution by nonlinear, slope-dependent transport: Steady state morphology and equilibrium adjustment timescales: Journal of Geophysical Research, v. 106, p. 16499-16513.

Roering, J.J., Kirchner, J.W., Sklar, L.S., and Dietrich, W.E., 2001b, Hillslope evolution by nonlinear creep and landsliding: An experimental study: Geology, v. 29, p. 143-146.

Roering, J.J.a.G., M., 2005, Fire and the evolution of steep, soil-mantled landscapes: Geology, v. 33, p. 349-352.

Small, E.E., Anderson, R.S., and Hancock, G.S., 1999, Estimates of the rate of regolith production using ^{10}Be and ^{26}Al from an alpine hillslope: Geomorphology, v. 27, p. 131-150.

Wells, N.A., and Andriamihaja, B., 1993, The initiation and growth of gullies in Madagascar: are humans to blame?: Geomorphology, v. 8, p. 1-46.

Willet, S.D., Brandon, M.T., 2002, On steady states in mountain belts: Geology, v. 30, p. 175-178.

Young, A., 1960, Soil movement by denudational processes on slopes: Nature, v. 188, p. 120-122.

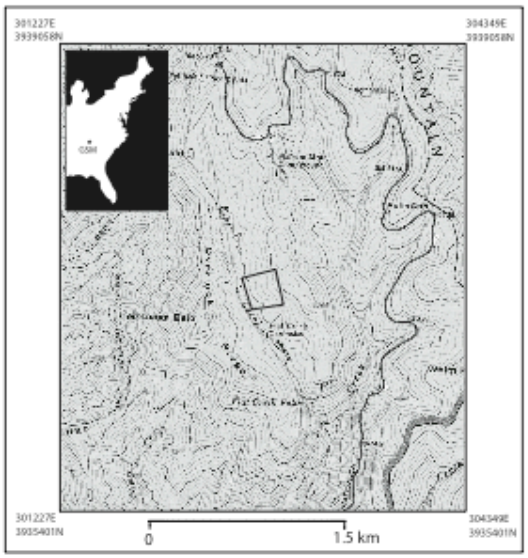
301227E
3939058N
304349E
3939058N
301227E
3935401N
304349E
3935401N
0
1.5 km

Figure 1

Figure 2a

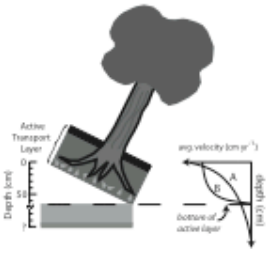

Figure 2b

Figure 3a.

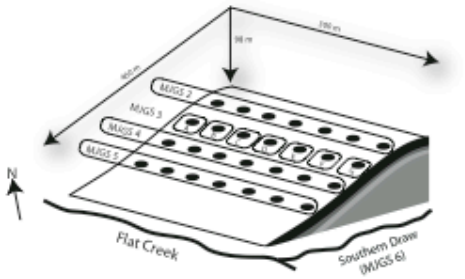

Figure 3b.

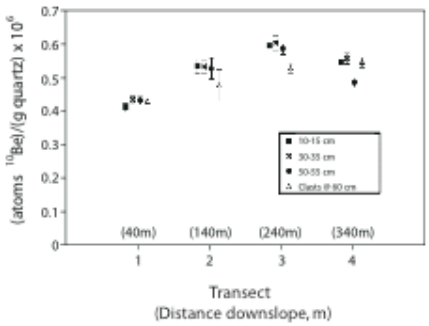

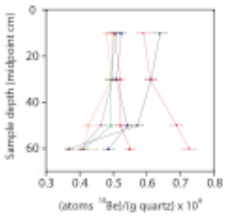

Figure 4a

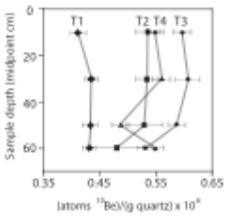

Figure 4b

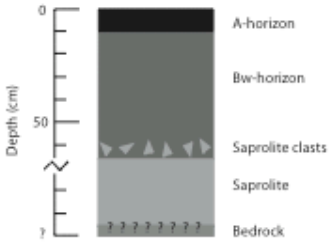

Figure 4c

Data Repository: Parameters for Soil Mass Balance and ^{10}Be Accumulation

We use a simple mass balance model to evaluate how parameters controlling soil flux would allow the accumulation of ^{10}Be that we observe in our samples. Soil mass at any point downslope is assumed to have come from either soil production from the underlying bedrock or from upslope positions. This soil is uniformly mixed within an active transport layer of either constant or incrementally increasing thickness with distance downslope. ^{10}Be abundances are achieved through *in situ* nuclide production, and inheritance of ^{10}Be from both upslope soil and from soil produced from underlying bedrock.

Initial conditions for the model are derived from both field observations and measured ^{10}Be concentrations. Soil at the hillcrest can only be sourced from underlying bedrock, and its ^{10}Be concentration should be proportional to measured abundances from weathered clasts at T1. The average rate of soil mass production on the hillslope was calculated to be 0.0018 $g \cdot cm^{-2} \cdot yr^{-1}$ based on a surface production rate of 15.03 $atoms \cdot yr^{-1}$ and an average soil density of 1.1 $g \cdot cm^{-3}$ (Heimsath et al., 1997). An initial thickness for the active transport layer of 55 cm is based on both field observations of tree throw patterns and patterns of ^{10}Be abundance vs. sample depth. A soil velocity of 1 $cm \cdot yr^{-1}$ at T1 is inferred from the distance between transects and the pattern of ^{10}Be accumulation between T1-T2 and T2-T3.

Soil flux must increase downslope, and our model accommodates for this increase in two ways; 1) increasing soil velocity downslope while keeping the thickness of the active transport layer constant, or 2) increasing the thickness of the active transport layer

downslope while keeping soil velocity constant. By manipulating these two parameters, we successfully fit curves for predicted ^{10}Be accumulation to our measured values for T1-T3. The drop in ^{10}Be concentrations at T4 remains enigmatic, as stated in the text.

REFERENCES CITED

Heimsath, A.M., Dietrich, W.E., Nishiizumi, K., and Finkel, R.C., 1997, The soil production function and landscape equilibrium: Nature (London), v. 388, p. 358-361.

CHAPTER 5: CONCLUSIONS

The methods presented in this thesis represent innovation both in the field of cosmogenics and in the quantification of hillslope processes. Data show that our methodological assumptions are sound, and our sampling protocol is easily adapted to different environments. *In situ*-produced ^{10}Be is unique as a geomorphic tracer because not only can it be used to track the movement of soil downslope, but its abundance is also linked to the rate of soil production from underlying bedrock. This link was very important for our development of a soil mass balance model for the Great Smoky Mountains hillslope. By sampling at several depths along each transect, we gain insight into soil velocity depth profiles and small scale hillslope processes such as soil mixing depth. In the Great Smoky Mountains, ^{10}Be concentrations depth profiles suggested efficient mixing to a depth of at least 55 cm. This isotopic evidence was supported by field observations of tree throw events that routinely turned soil over to a depth of 60 cm. In contrast, our data from Madagascar do not support a similar style of soil mixing, which is not surprising given the lack of deeply rooting vegetation on that hillslope.

The results from the full dataset for the Great Smoky Mountains are consistent with quantified soil flux rates and diffusion coefficients from other studies. This project strove to develop a new method for quantifying the rates of hillslope processes that avoided conventional assumptions. We were successful in doing so, and by operating outside of those assumptions, we raised important questions about how hillslope erosion rates are commonly considered in an ancient mountain range such as the Appalachians.

While it has been posited that erosion has achieved a steady rate in the Appalachians (Matmon et al., 2003a; Matmon et al., 2003b), our results suggest that on hillslopes, short-term climatic variations can have important impacts on erosion rates. A change in dominant vegetation type or a change to periglacial conditions can have important feedbacks on the hillslope scale. If hillslope erosion rates are changing during these variations, then there must be some impact on patterns of river basin-scale erosion. By better defining the link between these two scales of erosion in a previously studied landscape, we successfully attained another stated goal of our research.

Our success in the Great Smoky Mountains seems to suggest that our methods are widely applicable; however in some environments more care must be taken to make sure that enough sample types are collected in order to fully inform any transport models. For example, in Madagascar, we were not able to sample at the soil-bedrock boundary, so we are not able to quantify a soil production rate from *in situ*-produced ^{10}Be. We will be able to quantify this rate at a later date pending the return of meteoric ^{10}Be concentrations for the same samples. The lesson learned is to either select sites where sampling conditions are amenable to the methods, or collect enough sample to determine the components of the hillslope's processes by several techniques.

This method of soil amalgamation along hillcrest-parallel transects is effective for determining soil production and transport rates across varied tectonic and climatic settings. Sample collection is labor-intensive, but the results are worth the effort. Rates can be quantified without relying on assumed links between hillslope gradient and soil flux, so this method is well-suited for testing previous assertions about soil transport laws

from previous studies. This work has also proven itself as useful when considering broader-scale interpretations of landscape evolution. Any study of river basin or mountain range scale erosion rates would be amiss to not seek the quantification of soil production and transport rates on hillslopes within its study area. After all, the hillslopes are where all sediment flux begins.

REFERENCES

Andrews, D.J., Buckman, R.C., 1975, Fitting degradation of shoreline scarps by a nonlinear diffusion model: Journal of Geophysical Research, v. 92, p. 12857-12867.

Bierman, P.R., Albrecht, A., Bothner, M., Brown, E., Bullen, T., Gray, L., and Turpin, L., 1998, Weathering, erosion and sedimentation, *in* Kendall, C., and McDonnell, J.J., eds., Isotope Tracers in Catchment Hydrology, Elsevier, p. 647-678.

Bierman, P.R., and Caffee, M., 2002, Cosmogenic exposure and erosion history of ancient Australian bedrock landforms: Geological Society of America Bulletin, v. 114, p. 787-803.

Bierman, P.R., Clapp, E.M., Nichols, K.K., Gillespie, A.R., and Caffee, M., 2001, Using cosmogenic nuclide measurements in sediments to understand background rates of erosion and sediment transport„ *in* Harmon, R.S., and Doe, W.M., eds., Landscape Erosion and Evolution Modelling: New York, Kluwer, p. 89-116.

Bierman, P.R., and Steig, E., 1996, Estimating rates of denudation and sediment transport using cosmogenic isotope abundances in sediment: Earth Surface Processes and Landforms, v. 21, p. 125-139.

Brown, E.T., Edmond, J.M., Raisbeck, G.M., Yiou, F., Kurz, M.D., and Brook, E.J., 1991, Examination of surface exposure ages of Antarctic moraines using in situ produced ^{10}Be and ^{26}Al: Geochimica et Cosmochimica Acta, v. 55, p. 2269-2283.

Brown, E.T., Stallard, R.F., Larsen, M.C., Raisbeck, G.M., and Yiou, F., 1995, Denudation rates determined from the accumulation of in situ-produced ^{10}Be in the Luquillo Experimental Forest, Puerto Rico: Earth and Planetary Science Letters, v. 129, p. 193-202.

Carson, M.A., Kirkby, M.J., 1972, Hillslope form and process: Cambridge University Press, New York, p. 475.

Daly, C., and Taylor, G., 1998, Pennsylvania Average Annual Precipitation, 1961-90 : Portland, Oregon, Water and Climate Center of the Natural Resources Conservation Service.

Davis, W.M., 1892, The convex profile of badland divides: Science, v. 20, p. 245.

—, 1899, The Geographical Cycle: The Geographical Journal, v. 14, p. 481-504.

Dietrich, W.E., Bellugi, D., Heimsath, A.M., Roering, J.J., Sklar, L., and Stock, J.D., 2003, Geomorphic transport laws for predicting landscape form and dynamics, in Wilcock, P., and Iverson, R., eds., Prediction in Geomorphology, Volume Geophysical Monograph 135: Washington, D.C., American Geophysical Union, p. 103-132.

Duncan, C., Masek, J., Bierman, P., Larsen, J., and Caffee, M., 2001, Extraordinarily high denudation rates suggested by ^{10}Be and ^{26}Al analysis of river sediments, Bhutan Himalayas: Geological Society of America Abstracts with Programs, v. 33.

Fleming, R.W., and Johnson, A.M., 1975, Rates of seasonal creep of silty clay soil: Q.J. Engineering Geology, v. 8, p. 1-29.

Gilbert, G.K., 1877, Geology of the Henry Mountains (Utah): US Geographical and Geological Survey of the Rocky Mountains Region, 160 pp.

—, 1909, The convexity of hilltops: Journal of Geology, v. 17, p. 344-350.

Gosse, J.C., and Phillips, F.M., 2001, Terrestrial in situ cosmogenic nuclides: theory and application: Quaternary Science Reviews, v. 20, p. 1475-1560.

Heimsath, A.M., Chappell, J., Spooner, N.A., and Questiaux, D., 2002, Creeping Soil: Geology, v. 30, p. 111-114.

Heimsath, A.M., Dietrich, W.E., Nishiizumi, K., and Finkel, R.C., 1997, The soil production function and landscape equilibrium: Nature (London), v. 388, p. 358-361.

—, 1999, Cosmogenic nuclides, topography, and the spatial variation of soil depth: Geomorphology, v. 27, p. 151-172.

—, 2001, Stochastic processes of soil production and transport; erosion rates, topographic variation and cosmogenic nuclides in the Oregon Coast Range: Earth Surface Processes and Landforms, v. 26, p. 531-552.

Heimsath, A.M., Furbish, D.J., and Dietrich, W.E., 2005, The illusion of diffusion: Field evidence for depth-dependent sediment transport: Geology, v. 33, p. 949-952.

Kirchner, J.W., Finkel, R.C., Riebe, C.S., Granger, D.E., Clayton, J.L., King, J.G., and Megahan, W.F., 2001, Mountain erosion over 10 yr, 10 k.y., and 10 m.y. time scales: Geology, v. 29, p. 591-594.

Lal, D., 1991, Cosmic ray labeling of erosion surfaces; in situ nuclide production rates and erosion models: Earth and Planetary Science Letters, v. 104, p. 424-439.

Lal, D., and Peters, B., 1967, Cosmic ray produced radioactivity on the earth, *in* Sitte, K., ed., Handbuch der Physik: New York, Springer-Verlag, p. 551-612.

Lekach, J., Amit, R., Grodek, T., Schick, A.P., 1998, Fluvio-pedogenic processes in an ephemeral stream channel, Nahal Yael, Southern Negev, Israel.: Geomorphology, v. 23, p. 353-369.

Martin, Y., Church, Michael, 1997, Diffusion in Landscape Development Models: On the Nature of Basic Transport Relations: Earth Surface Processes and Landforms, v. 22, p. 273-279.

Matmon, A., Bierman, P.R., Larsen, J., Southworth, S., Pavich, M., and Caffee, M., 2003a, Temporally and spatially uniform rates of erosion in the southern Appalachian Great Smoky Mountains: Geology, v. 31, p. 155–158.

Matmon, A.S., Bierman, P., Larsen, J., Southworth, S., Pavich, M., Finkel, R., and Caffee, M., 2003b, Erosion of an ancient mountain range, the Great Smoky Mountains, North Carolina and Tennessee: American Journal of Science, v. 303, p. 817-855.

McKean, J.A., Dietrich, W.E., Finkel, R.C., Southon, J.R., and Caffee, M.W., 1993, Quantification of soil production and downslope creep rates from cosmogenic 10Be accumulations on a hillslope profile: Geology, v. 21, p. 343-346.

Monaghan, M.C., McKean, J., Dietrich, W., and Klein, J., 1992, 10-Be chronometry of bedrock-to-soil conversion rates: Earth and Planetary Science Letters, v. 111, p. 483-492.

Nichols, K.K., Bierman, P.R., Hooke, R.L., Clapp, E., and Caffee, M., 2002, Quantifying sediment transport on desert piedmonts using ^{10}Be and ^{26}Al: Geomorphology, v. 45, p. 89-104.

Nishiizumi, K., Kohl, C.P., Arnold, J.R., Klein, J., Fink, D., and Middleton, R., 1991, Cosmic ray produced ^{10}Be and ^{26}Al in Antarctic rocks; exposure and erosion history: Earth and Planetary Science Letters, v. 104, p. 440-454.

Penck, W., 1953, Morphological analysis of landforms: London, MacMillian, p. 429.

Reneau, S.L., and Dietrich, W.E., 1991, Erosion rates in the southern Oregon Coast Range: evidence for an equilibrium between hillslope erosion and sediment yield: Earth Surface Processes and Landforms, v. 16, p. 307-322.

Roering, J.J., Almond, P., Tonkin, P., and McKean, J., 2002, Soil transport driven by biological processes over millennial time scales: Geology, v. 30, p. 1115-1118.

Roering, J.J., Kirchner, J.W., and Dietrich, W.E., 1999, Evidence for nonlinear, diffusive sediment transport on hillslopes and implications for landscape morphology: Water Resources Research, v. 35, p. 853-870.

—, 2001a, Hillslope evolution by nonlinear, slope-dependent transport: Steady state morphology and equilibrium adjustment timescales: Journal of Geophysical Research, v. 106, p. 16499-16513.

Roering, J.J., Kirchner, J.W., Sklar, L.S., and Dietrich, W.E., 2001b, Hillslope evolution by nonlinear creep and landsliding: An experimental study: Geology, v. 29, p. 143-146.

Roering, J.J.a.G., M., 2005, Fire and the evolution of steep, soil-mantled landscapes: Geology, v. 33, p. 349-352.

Schultz, A.P., 1999, The geology of Pennsylvania: Harrisburg, PA, Pennsylvania Geological Survey, p. 888.

Small, E.E., Anderson, R.S., and Hancock, G.S., 1999, Estimates of the rate of regolith production using ^{10}Be and ^{26}Al from an alpine hillslope: Geomorphology, v. 27, p. 131-150.

Wells, N.A., and Andriamihaja, B., 1993, The initiation and growth of gullies in Madagascar: are humans to blame?: Geomorphology, v. 8, p. 1-46.

Willet, S.D., Brandon, M.T., 2002, On steady states in mountain belts: Geology, v. 30, p. 175-178.

Young, A., 1960, Soil movement by denudational processes on slopes: Nature, v. 188, p. 120-122.

APPENDICES

Appendix 1 Additional Field Sites

My study sites were selected primarily because they are contained within basins with ^{10}Be-quantified erosion rates. This provides context for my data, and allows me to add to the overall understanding of landscape change within previously studied basins. General site characteristics and differences between different sites are contained in Table 1 and Table 2.

Table 1. General site characteristics.

Location	Average slope (degrees)	# of Transects	Transect Length (meters)	# of Samples
Pennsylvania	25	4	300	12
New Zealand	20	4	300	14
Great Smoky Mountains, TN	5-10	4	300	45
Oregon Coast Range	10-15	4	100	17
Madagascar	15-20	4	300	8

Table 2. Tectonic, lithologic, and climatic differences between study sites.

Location	Tectonic Setting	Lithology	Precipitation (m yr^{-1})	Erosion (m My^{-1})
Susquehanna Basin, PA, USA	ancient orogeny, now passive margin	sandstone	0.8-1.3	4.0-54
Waipoa Basin, Gisborne, NZ	active subduction	sandstone/ mudstone	1.5	1700
Great Smoky Mountains, NC, USA	ancient orogeny, now passive margin	sandstone	1.4-2.3	27 +/- 4
Oregon Coast Range, OR, USA	active subduction	sandstone	1.5	125-130
Amparafaravola, Madagascar	stable craton	granite/gneiss	1.0-2.0	12

Appendix 1.1 Amparafaravola, Central Plateau, Madagascar

Appendix 1.1.1 Setting

The central plateau of Madagascar ranges in elevation from 1000 to 2000 m with local relief between flat valleys and convex hillslopes of 100 to 500 m (Wells and Andriamihaja, 1993). Annual rainfall ranges from 100-200 cm, which is intermediate between the much wetter eastern rain forest and the arid southwest of the island (Donque and Rabenjy, 1972). The craton is composed of granites, migmatites, gneisses, and schists that are commonly covered by a thick lateritic regolith (Wells and Andriamihaja, 1993).

Appendix 1.1.2 Data

The dosing pattern for samples moving from upslope to downslope positions appears different for Madagascar than for the Smoky Mountains, but the Madagascar data are systematic, nonetheless, and are therefore amenable to modeling.

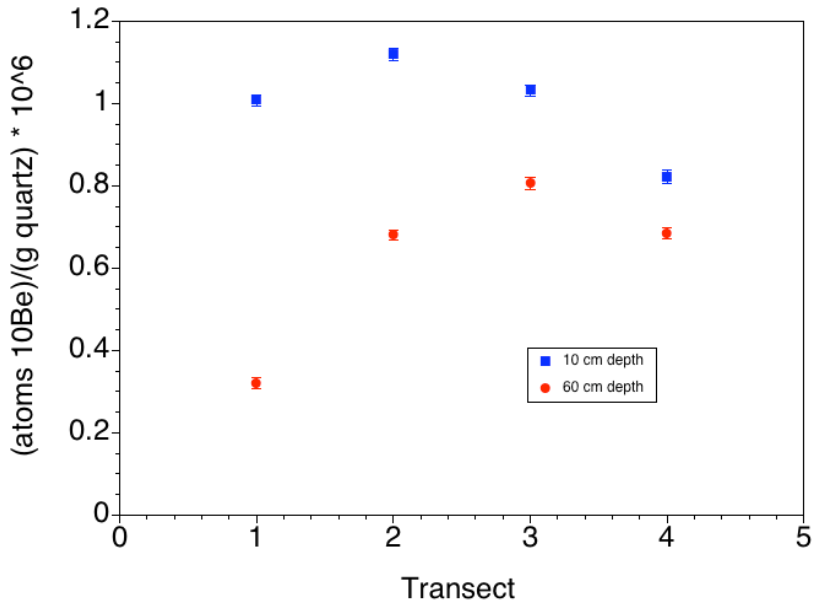

Figure 2. ^{10}Be concentrations for soil and bedrock samples from Amparafaravola, Madagascar. Concentrations of ^{10}Be increases then decreases systematically with distance downslope. Error bars represent 1σ analytical error

Disparate ^{10}Be concentrations for each transect's sample depths suggest that mixing processes are not as effective in Madagascar as they are in the Smoky Mountains (Figure 2). The absence of deep-rooting vegetation from this region of Madagascar is a possible explanation, and I did not see any evidence for 10-60 cm scale turnover while collecting these samples.

Appendix 1.2 Laurely Fork, Pennsylvania, USA

Appendix 1.2.1 Setting

We sampled a planar hillslope with a maximum elevation of 615 m, and a local relief of 220 m between the hillcrest and Laurely Fork, which is the lower boundary of the slope. The average gradient of the slope is 25^{o}, and the linear distance from the

hillslope's ridge to Laurely Fork is approximately 600 m. This hillslope is located within the Appalachian Plateau physiographic region of the Susquehanna Basin, which is underlain by relatively undeformed sedimentary bedrock, largely sandstone and shale. The Susquehanna Basin climate is humid and temperate, with mean annual precipitation ranging from about 0.8 to 1.3 meters, depending on location (Daly and Taylor, 1998). Phanerozoic mountain building events, followed by rifting in the Triassic/Jurassic created the passive margin that the Susquehanna River drains today (Schultz, 1999). Erosion rates for the Susquehanna Basin, based upon ^{10}Be concentrations in river sediment, range from 4-54 m My^{-1} (Reuter et al., accepted).

The slope is well-vegetated, with a thick forest canopy dominated by deciduous trees such as Northern red oak (*Quercus rubra*). The entire hillslope is armored by flat, sandstone clasts that are thought to be of periglacial origin (ref). Soil is found in the interstices of this clast matrix. These clasts collect behind trees, creating wedge-shaped reservoirs for large- and small-grained sediment. Tree throw is necessary for sediment to be released downslope. However, evidence for tree throw is limited to faint scars low on the slope. Other possible mechanisms for sediment transport are dry ravel of coarser grains, and the flushing of smaller grains through the clast matrix by flowing water.

Soil development is minimal on the slope, resulting in a general classification of the soils as entisols. This implies a short residence time for sand-sized grains. Soil colors were generally 10YR 5/4, and the texture of soils on the slope was almost universally a very fine sandy loam. Concentrations of soil were overlain by at least 5 cm

of the aforementioned periglacial armoring. The thickness of this armor increases downslope with maximum values of 20 cm encountered on our lowest sampling transect.

Appendix 1.2.2 Data

Concentrations of ^{10}Be decrease systematically with distance downslope (Figure 3). Thus, ^{10}Be is not accumulating in sand-sized grains as they are transported downslope. This implies that the transport rates for this sediment must be faster than the production rate of ^{10}Be in the grains themselves, and in the substrate from which the soil is being produced.

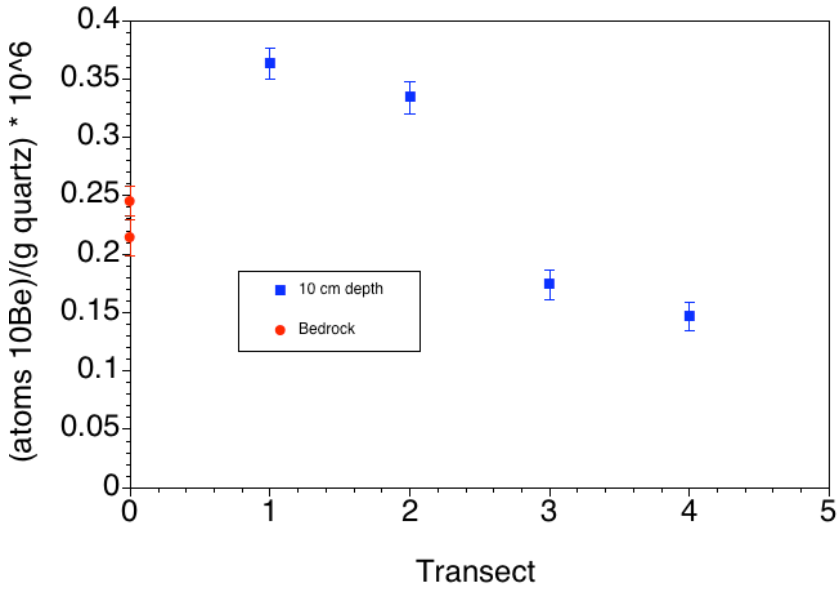

Figure 3. ^{10}Be concentrations for soil and bedrock samples from Laurely Fork, PA. Concentrations of ^{10}Be decrease systematically with distance downslope. Thus, ^{10}Be is not accumulating in sand-sized grains as they are transported downslope. ^{10}Be concentrations for bedrock outcrops (0.214 and 0.245 x 10^6 atoms·g^{-1}) at the top of the slope are intermediate compared to the soil samples. This supports inheritance of ^{10}Be from underlying bedrock for the upper two transects (MJPA1 and MJPA2). Error bars represent 1σ analytical error.

Pending measurements of ^{10}Be in coarser-grained clasts (>2 cm along the long-axis) should help to resolve differences in the transport rates of different grain-sizes on the slope, and whether soil is being produced from clasts or from underlying bedrock.

^{10}Be concentrations for bedrock outcrops (0.214 and 0.245 x 10^6 atoms·g^{-1}) at the top of the slope are intermediate compared to the soil samples. This supports inheritance of ^{10}Be from underlying bedrock for the upper two transects (MJPA1 and MJPA2). The low ^{10}Be concentrations for the lowest two transects (MJPA5 and MJPA6) could be the result of soil formation from shielded bedrock or periglacial cobbles. The pending analysis of the remaining samples from this site is crucial for any further insight into hillslope processes in this environment.

Appendix 1.3 Waipaoa River Basin, North Island, New Zealand

Appendix 1.3.1 Setting

The Waipaoa River drains into Poverty Bay on the east coast of New Zealand's North Island. Annual rainfall averages 1.5 m (http://baby.indstate.edu/gomez/margins.html; 2/05). The bedrock in the basin's headwaters is composed of highly crushed Cretaceous and Paleocene mudstones and argillites (DeRose et al., 1998), while the lower Waipaoa is underlain by poorly consolidated sandstone and mudstones of Miocene and Pliocene age (Gage and Black, 1979). This basin is situated within the active forearc margin of the Hikurangi subduction margin, and is undergoing broad regional uplift on the order of 0.5-1.1 mm/yr (Berryman et al., 2000). Long-term sediment yields for the Waipaoa River

Basin and its tributaries have been estimated to be as high as 1700 m My^{-1} (Hicks et al., 2000).

Appendix 1.3.2 Data

There are currently no data available for this field site.

Appendix 1.4 Coast Range, Oregon, USA

Appendix 1.4.1 Setting

The Oregon Coast Range is a tectonically active, deeply dissected mountain range that runs north-south in western Oregon. The climate is temperate and wet with >2 m of precipitation annually (http://www.wrh.noaa.gov/images/pqr/prec_OR.gif; 3/05), and is underlain by a relatively undeformed sequence of lithic Eocene turbidite sandstone, the Tyee Formation (Snavely et al., 1964; Lovell, 1969; Heller et al., 1985). This bedrock is extensively weathered and fractured with saprolite depths of several meters in some places (Heimsath et al., 2001). Rock uplift rates have been estimated at between 30 and 230 m Ma^{-1} through the dating of marine terraces (Kelsey and Bockheim, 1994; Kelsey et al., 1994). Erosion rates for the Drift Creek basin within the Oregon Coast Range have been measured at 125-130 m My^{-1} (Bierman et al., 2001), consistent with but not mandating approximate equilibrium between uplift and erosion (Reneau and Dietrich, 1991).

Appendix 1.4.2 Data

There are currently no data available for this field site.

Appendix 2 ^{10}Be Data and Sample Locations

^{10}Be data and sample locations

Sample ID	Sample Location	Sample Type	Sample Depth	UTM Zone	Easting	Northing	Measured 10Be Concentration
			cm				10^6 atoms g^{-1}
MJGS2	Great Smoky Mountains, NC			17S	302854-302948	3937232-3936973	
		soil	10-15				0.412 ± 0.0134
		soil	30-35				0.435 ± 0.0116
		soil	50-55				0.434 ± 0.0128
		clast	~60				0.432 ± 0.0115
MJGS3	Great Smoky Mountains, NC						
A		soil	10-15	17S	302771	3937230	0.524 ± 0.0134
		soil	30-35				0.509 ± 0.0142
		soil	50-55				0.542 ± 0.0142
		clast	~60				0.486 ± 0.0166
B		soil	10-15	17S	302767	3937185	0.504 ± 0.0133
		soil	30-35				0.520 ± 0.0133
		soil	50-55				0.521 ± 0.0143
		clast	~60				0.550 ± 0.0141
C		soil	10-15	17S	302799	3937141	0.508 ± 0.0131
		soil	30-35				0.492 ± 0.0139
		soil	50-55				0.494 ± 0.0127
		clast	~60				0.412 ± 0.0122
D		soil	10-15	17S	302809	3937096	0.501 ± 0.0128
		soil	30-35				0.498 ± 0.0157
		soil	50-55				0.463 ± 0.0144
		clast	~60				0.406 ± 0.0122
E		soil	10-15	17S	302798	3937042	0.481 ± 0.0129
		soil	30-35				0.496 ± 0.0135
		soil	50-55				0.426 ± 0.0109
		clast	~60				0.411 ± 0.0430
F		soil	10-15	17S	302807	3937009	0.638 ± 0.0196
		soil	30-35				0.612 ± 0.0160
		soil	50-55				0.571 ± 0.0176
		clast	~60				0.369 ± 0.0123
G		soil	10-15	17S	302832	3936908	0.590 ± 0.0184
		soil	30-35				0.609 ± 0.0159
		soil	50-55				0.687 ± 0.0185
		clast	~60				0.725 ± 0.0185
MJGS4	Great Smoky Mountains, NC			17S	302758-302689	3936944-3937193	
		soil	10-15				0.596 ± 0.0160
		soil	30-35				0.606 ± 0.0217
		soil	50-55				0.587 ± 0.0152
		clast	~60				0.530 ± 0.0141
MJGS5	Great Smoky Mountains, NC			17S	302678-302608	3936894-3937142	
		soil	10-15				0.548 ± 0.0147
		soil	30-35				0.560 ± 0.0161
		soil	50-55				0.487 ± 0.0151
		clast	~60				0.548 ± 0.0154
MJGS6	Great Smoky Mountains, NC			17S	302635	3936883	0.719 ± 0.0185
		sediment from					
A		southern draw	surface				
B		quartz clast	surface				0.684 ± 0.0178
C		gneiss clast	surface				0.555 ± 0.0155
D		quartzite clast	surface				0.539 ± 0.0141
MG1`	Amparafaravola, Madagascar			38S	819136-819117	8095845-8095844	
A		soil	10-15				1.007 ± 0.0246
B		soil	55-60				0.320 ± 0.0104

GPS points collected with a Garmin 75 handheld unit; Great Smoky Mountain, Pennsylvania, and Oregon samples are reported in NAD 83, New Zealand and Madagascar samples are reported in WGS 84.

^{10}Be data and sample locations

Sample ID	Sample Location	Sample Type	Sample Depth	UTM Zone	Easting	Northing	Measured	10Be	Concentration
			cm				10^6 atoms g^{-1}		
	Amparafaravola,				819192-	8095800-			
MG2	Madagascar			38S	819281	8095781			
A		soil	10-15				1.119 ±		0.0274
B		soil	55-60				0.680 ±		0.0218
	Amparafaravola,				819233-	8095757-			
MG3	Madagascar			38S	819253	8095717			
A		soil	10-15				1.031 ±		0.0252
B		soil	55-60				0.806 ±		0.0197
	Amparafaravola,				819268-	8095798-			
MG4	Madagascar			38S	819214	8095726			
A		soil	10-15				0.821 ±		0.0201
B		soil	55-60				0.684 ±		0.0214
MJPA1	Laurely Fork, PA						0.363 ±		0.0122
A		soil	10-15						
B		clast	10-15						
MJPA2	Laurely Fork, PA			18N	268841	4572810			
A		soil	10-15				0.334 ±		0.0127
B		clast	10-15						
MJPA3	Laurely Fork, PA	bedrock					0.214 ±		0.015708608
MJPA4	Laurely Fork, PA	bedrock					0.245 ±		0.012825317
MJPA5	Laurely Fork, PA			18N	268630	4572721			
A		soil	10-15				0.174 ±		0.0139
B		clast	10-15						
MJPA6	Laurely Fork, PA								
A		soil	10-15				0.147 ±		0.0131
B		clast	10-15						
MJPA7	Laurely Fork, PA								
A		river sediment	surface						
B		river clast	surface						
	North Island, New				2925636-	6263645-			
MJNZ1	Zealand			NZ Grid	2925417	6263744			
A		soil							
B		soil							
	North Island, New				2925592-	6263500-			
MJNZ2	Zealand			NZ Grid	2925381	6263681			
A		soil							
B		soil							
	North Island, New				2925533-	6263457-			
MJNZ3	Zealand			NZ Grid	2925353	6263617			
A		soil							
B		soil							
	North Island, New				2925468-	6263398-			
MJNZ4	Zealand			NZ Grid	2925314	6263526			
A		soil							
B		soil							
	North Island, New								
MJNZ5-10	Zealand			NZ Grid	2925500	6263626			
5		soil							
6		soil							
7		soil							
8		soil							
9		soil							
10		soil							
	Oregon Coast				425318-	4922568-			
MJOR1	Range, OR			10N	425511	4922487			
		soil							
		soil							
		soil							
		clast							
	Oregon Coast				425323-	4922634-			
MJOR2	Range, OR			10N	425531	4922518			
		soil							
		soil							
		soil							
		clast							
	Oregon Coast				425399-	4922670-			
MJOR3	Range, OR			10N	425567	4922573			
		soil							
		soil							
		soil							
		clast							
	Oregon Coast				425364-	4922771-			
MJOR4	Range, OR			10N	425588	4922654			
		soil							
		soil							
		soil							
		clast							

GPS points collected with a Garmin 75 handheld unit; Great Smoky Mountain, Pennsylvania, and Oregon samples are reported in NAD 83, New Zealand and Madagascar samples are reported in WGS 84.